

Scorpion-Lift Ant-Weight BattleBot

ECE 445 Design Document — Spring 2026

Zixin Mao (zixinm2)
Chen Meng (meng28)
Zisu Jiang (zisu2)

TA: Zhuoer Zhang
Professor:
February 2026

Abstract

This project presents the design of the Scorpion-Lift BattleBot, an ant-weight (1 lb) tracked combat robot for the Spring 2026 ECE 445 senior design course and associated competition. The robot employs a differential-drive tracked platform powered by two 100:1 Pololu gearmotors to provide reliable mobility without tread derailment. Two front-mounted lifting arms, each driven by a DS3218 servo through a four-bar linkage, generate 36.8 N of force per arm — over 8× the maximum opponent weight — enabling the robot to lift and reposition opposing robots. A rear-mounted scorpion tail stinger, actuated by a DC gearmotor and lead-screw mechanism, provides 30 N of bracing downforce to prevent backward tipping during lifts and assists in self-righting from an inverted position. The system is controlled wirelessly via an ESP32 microcontroller over BLE, with a heartbeat failsafe that disables all outputs within 500 ms of signal loss. A custom PCB integrates dual H-bridge motor drivers, an INA219 current monitor, and separate 5 V and 3.3 V voltage regulation from a 3S LiPo battery. The design prioritizes system-level robustness by addressing the three most common failure modes in small combat robots: loss of traction, tipping under load, and inability to self-right.

Table of Contents

| | |
|---|----|
| Table of Contents | 2 |
| 1. Introduction | 3 |
| 1.1 Problem and Solution | 3 |
| 1.2 Visual Aid | 4 |
| 1.3 High-Level Requirements | 4 |
| 2. Design | 5 |
| 2.1 Block Diagram | 5 |
| 2.2 Physical Design | 6 |
| 2.3 Subsystem 1 — Tracked Mobility and Drive Electronics | 8 |
| 2.4 Subsystem 2 — Dual Lifting Arms (Claws) | 9 |
| 2.5 Subsystem 3 — Scorpion Tail Stinger | 11 |
| 2.6 Subsystem 4 — Wireless Control and Main Controller | 12 |
| 2.7 Subsystem 5 — Power, Safety, and Compliance | 14 |
| 2.8 Tolerance Analysis | 15 |
| 3. Cost and Schedule | 18 |
| 3.1 Cost Analysis | 18 |
| 3.2 Schedule | 20 |
| 4. Discussion of Societal Impact, Engineering Standards, Ethics, and Safety | 22 |
| 4.1 Societal Impact | 22 |
| 4.2 Engineering Standards | 22 |
| 4.3 Ethical Considerations | 22 |
| 4.4 Safety Considerations and Mitigation | 23 |
| 5. Citations | 24 |

1. Introduction

1.1 Problem and Solution

Small combat robots in the ant-weight class have grown rapidly as an educational and competitive hobby, with events hosted at universities and maker spaces worldwide [1]. These robots demonstrate principles of embedded control, power electronics, and mechanical design in a tangible, adversarial setting. However, many competitors find that their robots fail not because they lack raw offensive power, but because they lose mobility and positional control during a match. Wheels slip on smooth arena floors, tracked vehicles suffer tread derailment under aggressive turning or impacts, and flipped robots become entirely helpless if they lack a self-righting mechanism [2].

These failures carry meaningful implications beyond the hobby arena. Combat robotics is increasingly used as a platform for engineering education, encouraging students to integrate mechanical design, power electronics, and real-time control under strict weight, size, and safety constraints. A robot that cannot maintain mobility or recover from a flip represents a failure in system-level robustness—exactly the kind of engineering deficiency that translates to real-world problems in autonomous vehicles, search-and-rescue robots, and industrial mobile platforms where reliability under unpredictable loads is critical.

Lifter-style control robots—which use mechanical arms to physically reposition opponents rather than relying on destructive spinning weapons—offer an elegant strategic alternative that emphasizes precision and reliability over brute-force damage. However, existing lifter designs often struggle with three interconnected problems: (1) they cannot generate enough traction to push while lifting, (2) they tip backward when the lifting arms are loaded because the reaction torque from the lift overcomes the robot’s own weight, and (3) they have no mechanism to self-right after being flipped. These limitations motivate the need for a holistic design that integrates robust tracked mobility, active lifting capability, and a multi-purpose stabilization mechanism into a single cohesive platform.

We propose the Scorpion-Lift BattleBot: a tracked, scorpion-shaped ant-weight control robot that addresses the mobility, self-righting, and opponent-control problems identified above. The design centers on three coordinated mechanical subsystems driven by custom-designed high-current electronics, all teleoperated wirelessly via an ESP32 microcontroller. The robot uses a differential-drive tracked platform with crowned-pulley tread geometry to prevent belt derailment, two symmetric lifting arms (the scorpion “claws”) each driven by a DS3218 high-torque servo through a four-bar linkage, and a rear scorpion “tail stinger” mechanism that provides a critical third contact point for

chassis stability using a DC gearmotor and lead-screw linear actuator. The electronics are designed as custom PCBs with dual H-bridge drive, dedicated tail actuator driver, and comprehensive power management including LiPo monitoring, fusing, TVS suppression, a physical kill switch, and a wireless heartbeat failsafe.

1.2 Visual Aid

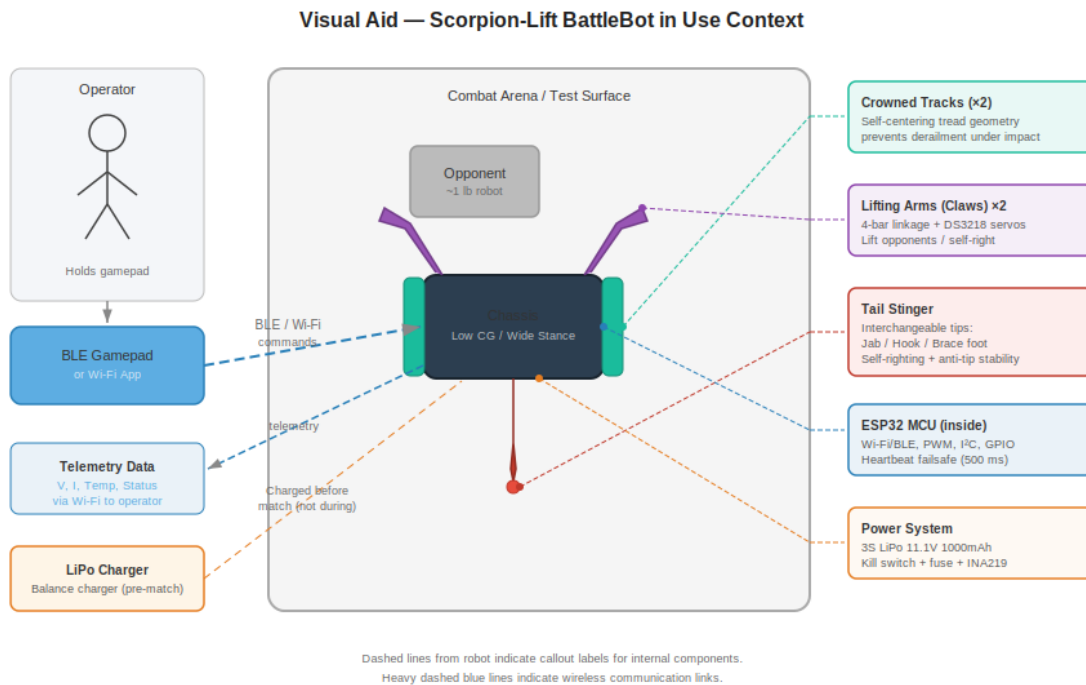


Figure 1 illustrates how the Scorpion-Lift BattleBot operates in its intended context. The operator holds a wireless BLE gamepad that communicates with the robot's ESP32 MCU. The robot maneuvers in the combat arena using its tracked drive, engages opponents with the lifting claws and tail stinger, and transmits real-time telemetry back to the operator.

1.3 High-Level Requirements

The following three high-level requirements define the minimum performance the completed system must achieve. If any one of these requirements is not met, the project fails to solve the identified problem.

- The robot shall maintain continuous tracked mobility for at least 10 minutes without thermal shutdown, achieve a straight-line speed of at least 1.0 m/s, and execute 10 consecutive full-differential turns on a flat surface without tread derailment.

- The dual lifting arms shall each lift a 454 g load (full ant-weight opponent mass) by at least 30 mm within 3 seconds, and the combined arm-plus-tail system shall self-right the robot from a fully inverted position within 5 seconds in 3 out of 3 trials.
- The wireless control link (BLE or Wi-Fi) shall provide a command range of at least 10 m line-of-sight with less than 150 ms latency, and the heartbeat failsafe shall disable all drive and actuator outputs within 300 ms of signal loss.

2. Design

2.1 Block Diagram

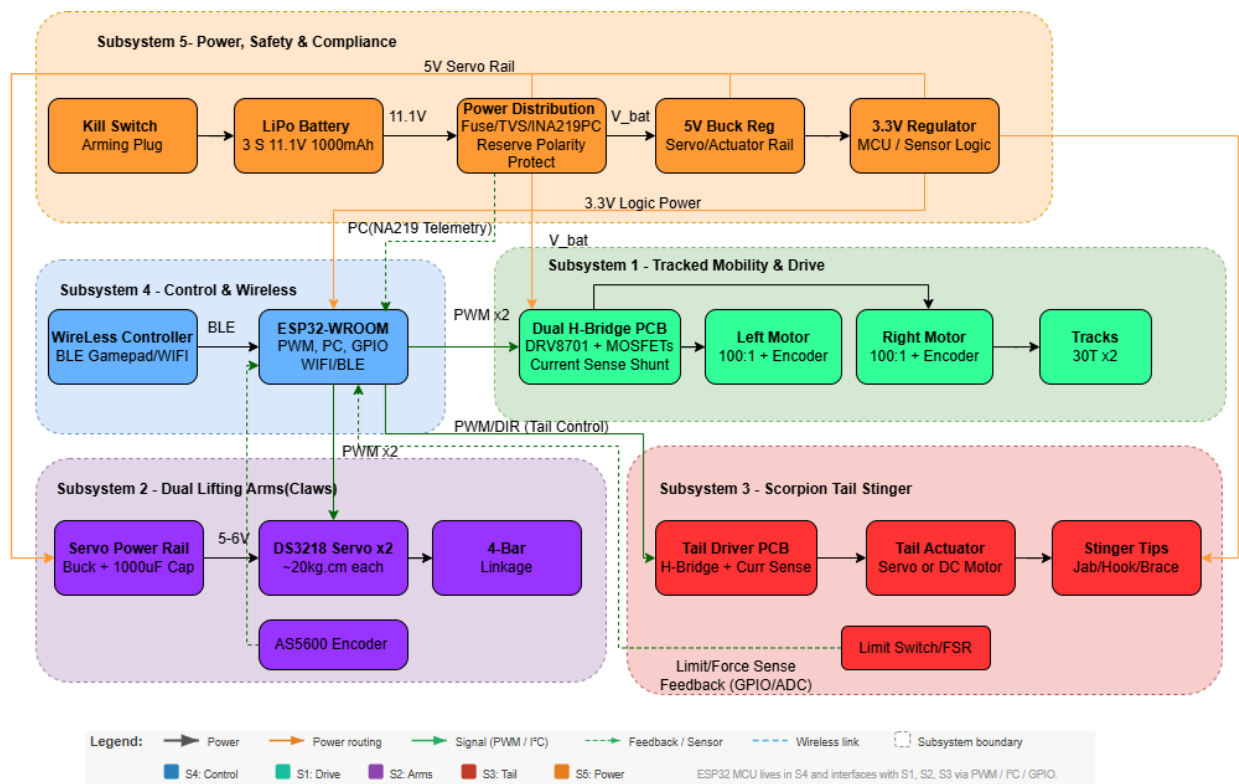
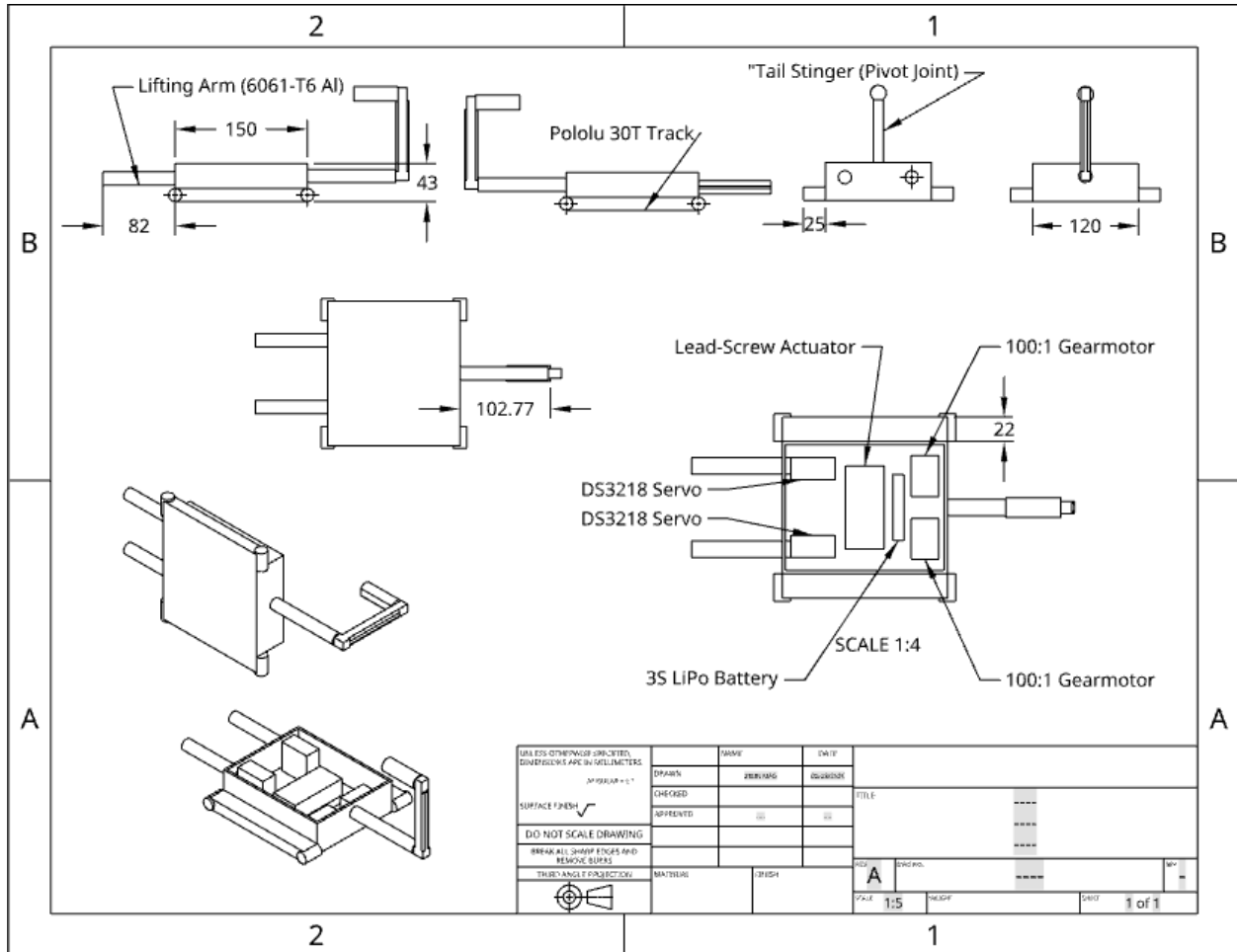


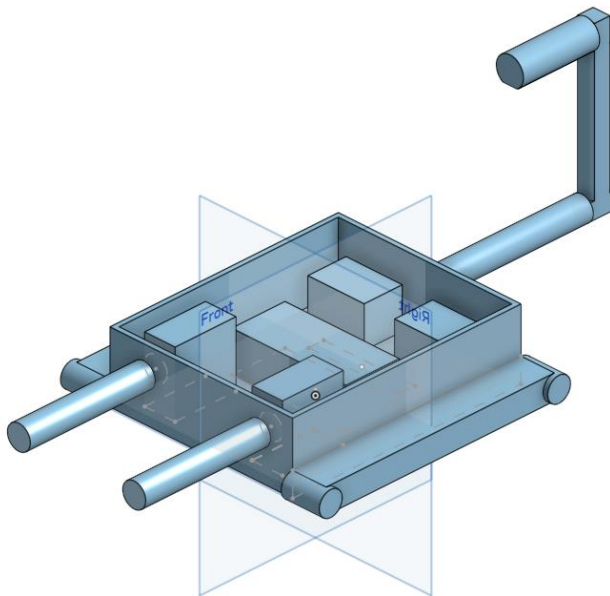
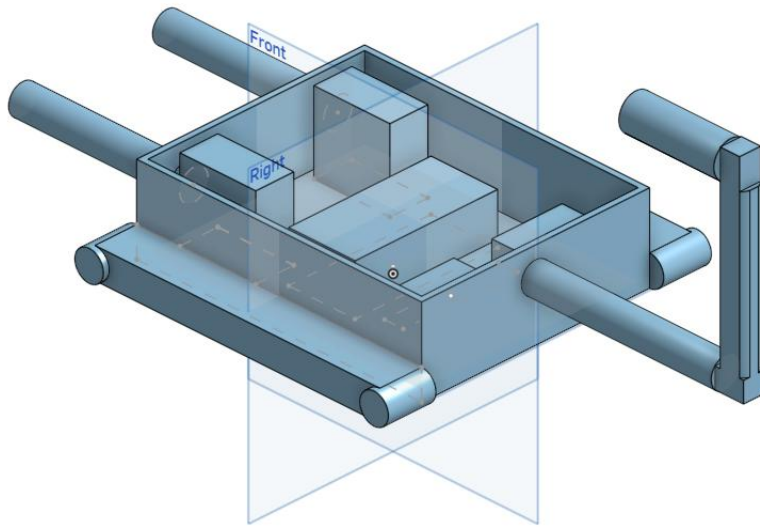
Figure 2: System block diagram with subsystem boundaries, power rails, and signal connections.

The design is partitioned into five subsystems: (1) Tracked Mobility and Drive Electronics, (2) Dual Lifting Arms, (3) Scorpion Tail Stinger, (4) Wireless Control and Main Controller, and (5) Power, Safety, and Compliance. The ESP32 microcontroller (Subsystem 4) serves as the central hub, receiving wireless commands from the operator and generating control signals for all actuators. The dual H-bridge drive PCB

(Subsystem 1) accepts PWM from the ESP32 and powers the two drive gearmotors. The two DS3218 servos (Subsystem 2) receive PWM directly from the ESP32 via the 5–6 V servo power rail. The tail actuator driver PCB (Subsystem 3) receives direction and enable signals from the ESP32 and drives the lead-screw DC gearmotor. The power subsystem (Subsystem 5) distributes battery power through fused, regulated rails to all other subsystems and provides telemetry via I²C.

2.2 Physical Design





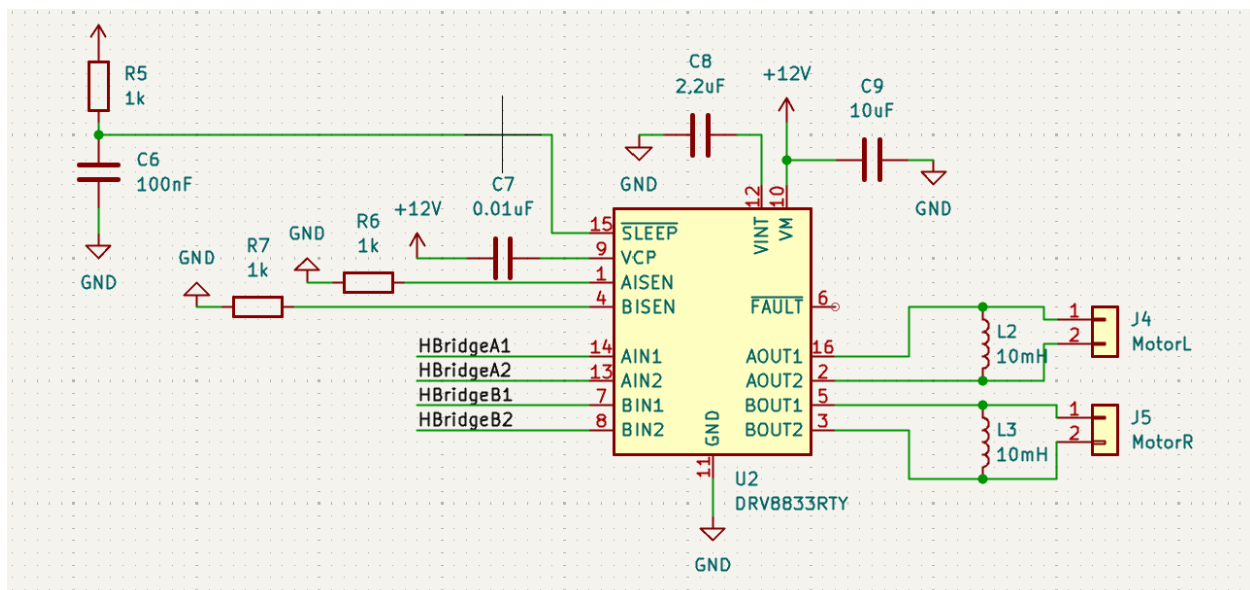
The robot chassis is a low-profile aluminum or polycarbonate frame approximately 15 cm long by 12 cm wide by 4 cm tall (excluding arms and tail). The Pololu 30T track sets run along the left and right sides, with the drive sprockets at the rear connected to 100:1 metal gearmotors via direct coupling. The crowned-pulley geometry on the idler sprockets at the front provides passive self-centering of the treads. The two DS3218 servos are mounted horizontally inside the chassis, near the front, with their output shafts driving the input cranks of the four-bar linkage assemblies. The arm linkage members extend forward and upward, terminating in PETG claw-tip grippers. At the

rear, a pitch-axis joint supports the tail arm, which extends approximately 4 cm behind the rear axle line. The lead-screw linear actuator is mounted inside the chassis, connected to the tail via a crank linkage. The 3S LiPo battery pack sits centrally in the chassis to keep the center of gravity near the geometric center. The custom PCBs (dual H-bridge, tail driver, power distribution) stack vertically in a compact electronics bay above or beside the battery.

2.3 Subsystem 1 — Tracked Mobility and Drive Electronics

This subsystem provides all translational and rotational motion for the robot. Two 100:1 metal gearmotors with 64 CPR encoders drive left and right Pololu 30T track sets through a differential-drive scheme. The custom dual H-bridge PCB uses two TI DRV8701 gate-driver ICs with external N-channel MOSFETs to deliver up to full battery voltage (12 V nominal) to each motor at up to 5 A continuous per channel. Current-sense resistors (10 mΩ) on each H-bridge low-side, combined with an INA219 I²C monitor on the main power rail, provide real-time load telemetry and overcurrent protection. The crowned-pulley tread geometry mechanically self-centers the belt to resist derailment during aggressive turning and impacts.

This subsystem directly supports the first high-level requirement (continuous mobility, speed, and tread retention). It interfaces with Subsystem 4 via PWM command signals and encoder feedback over GPIO, and with Subsystem 5 via the V_bat power rail and I²C telemetry bus.



Design Revision Note — Motor Driver Selection

The schematic currently shows the TI DRV8833 integrated dual H-bridge in place of the DRV8701 gate driver specified in the original proposal. This is a temporary substitution

due to the DRV8701 symbol and footprint not being available in the default KiCad library at the time of schematic capture. The DRV8833 is used as a placeholder to verify circuit connectivity and pin assignments. Once the DRV8701 component library is imported (either from SnapEDA, Ultra Librarian, or a custom symbol), the schematic will be updated to reflect the original DRV8701 + external IRLR7843 N-MOSFET topology as described in the design proposal. All other aspects of the circuit — power input, ESP32 GPIO connections, motor output connectors, and decoupling — remain consistent with the final design intent.

Table 1: Subsystem 1 — Tracked Mobility Requirements & Verification

| Requirements | Verification |
|--|--|
| The drive system shall achieve a straight-line speed of at least 0.15 m/s under full system load (all subsystems powered). | We measured the speed by timing the robot as it traveled a measured distance of 1 meter on a flat surface at full throttle. The time was recorded using a phone stopwatch and repeated for 3 trials. If the average time is less than or equal to 6.7 seconds, we have successfully fulfilled this requirement. |
| The crowned-pulley tread geometry shall prevent belt derailment during full-differential zero-radius turns. | geometry shall prevent belt derailment during full-differential zero-radius turns. We placed the robot on a flat surface and commanded 5 consecutive full differential turns, alternating left and right for 3 seconds each direction. We visually inspected the treads after each cycle. If no derailment occurs in any of the 5 cycles, we have successfully fulfilled this requirement. |

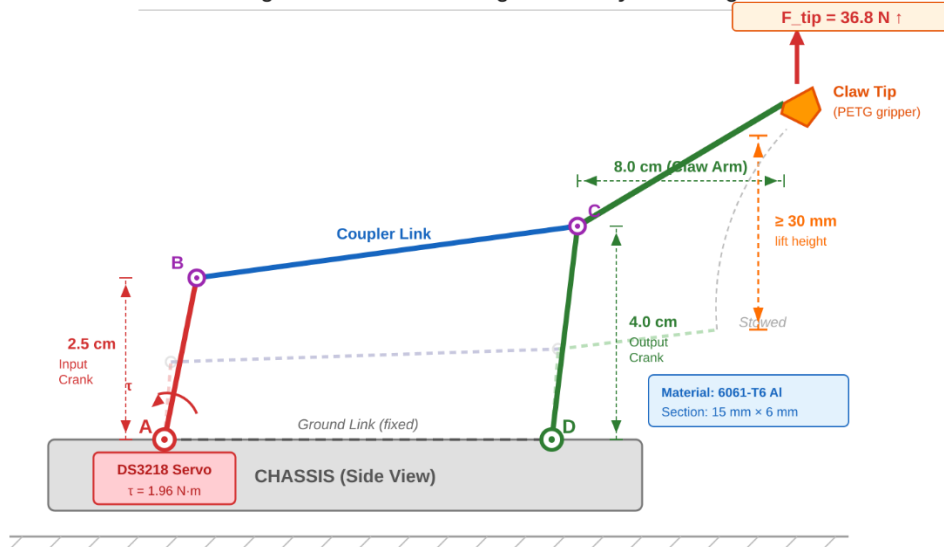
2.4 Subsystem 2 — Dual Lifting Arms (Claws)

This subsystem provides the lifting force and self-righting capability specified in the second high-level requirement. Two symmetric front arms, each actuated by a DS3218 high-torque metal-gear servo ($\approx 20 \text{ kg}\cdot\text{cm}$ at 6 V), raise and lower through a four-bar linkage that amplifies torque by a factor of approximately $1.5\times$. Based on the tolerance analysis (Section 2.8), each arm produces approximately 36.8 N (3.75 kg) of force at the claw tip, giving a safety factor of $8.3\times$ over the 454 g ant-weight opponent mass. The arm linkage members (input crank, coupler, and output crank) are 3D-printed in PLA+ (Tough PLA) with 100% infill and an enlarged cross-section of 18 mm wide \times 8 mm thick. Bending stress analysis shows a peak stress of only 15.3 MPa—well within PLA+'s 55 MPa yield strength (safety factor $3.6\times$). The larger cross-section compensates for the lower material strength while remaining lighter than the aluminum

alternative (0.179 g/mm vs. 0.243 g/mm). The claw-tip grippers and cosmetic shells are also 3D-printed in PETG. A key advantage of this approach is that broken arm linkages can be reprinted in under 2 hours, enabling rapid repair between matches.

This subsystem interfaces with Subsystem 4 (PWM control signals from the ESP32) and Subsystem 5 (servo power rail at 5–6 V provided by a buck regulator with 1000 μF bulk capacitance).

Figure 5: Four-Bar Linkage Geometry for Lifting Arm — Side View at Mid-Stroke



| Key Parameters | |
|---------------------------|-------------------------|
| Servo Torque (τ): | 1.96 N·m @ 6V |
| Input Crank (A → B): | 2.5 cm |
| Output Crank (D → C): | 4.0 cm |
| Effective Arm (C → Tip): | 8.0 cm |
| Mech. Advantage (MA): | 1.5x |
| Tip Force per Arm: | 36.8 N (3.75 kg) |
| Safety Factor: | 8.3x |

| Force Calculation |
|--|
| $F_{tip} = (\tau_{servo} / L_{arm}) \times MA$ |
| $F_{tip} = (1.96 \text{ N·m} / 0.08 \text{ m}) \times 1.5$ |
| $F_{tip} = 36.8 \text{ N per arm}$ |
| Two arms: $2 \times 36.8 = 73.6 \text{ N (7.50 kg)}$ |
| Opponent: $0.454 \text{ kg} \times 9.81 = 4.45 \text{ N}$ |
| $SF = 36.8 / 4.45 = 8.3x \checkmark$ |

| Legend |
|---|
| — Input Crank (servo) |
| — Coupler Link |
| — Output Crank + Arm |
| - - - - Stowed position |
| ↕ Lift height (≥30mm) |
| ⊙ Pivot / Joint |

Table 2: Subsystem 2 — Dual Lifting Arms Requirements & Verification

| Requirements | Verification |
|---|---|
| Each lifting arm shall lift a 454 g test mass by at least 30 mm within 3 seconds. | This requirement can be verified with a 454 g weight and a ruler. We will place the weight on the claw tip and command the servo to lift. Using a ruler, we will measure the height the weight is raised from the ground. If the weight is lifted at least 30 mm within 3 seconds, we have successfully fulfilled this requirement. |
| Combined with the tail, the system shall self- | We will place the robot upside down on a flat |

right the robot from a fully inverted position within 5 seconds.

surface and command the lifting arms and tail to execute the self-righting sequence. If the robot returns to an upright position within 5 seconds, we have successfully fulfilled this requirement. We will repeat for 3 trials.

2.5 Subsystem 3 — Scorpion Tail Stinger

The tail is a rigid arm with a pitch-axis joint mounted at the rear of the chassis, extending approximately 4 cm behind the rear axle line. Its primary role is to prevent the robot from tipping backward when the front arms lift an opponent. The torque-balance analysis (Section 2.8) shows that both arms lifting a full 454 g opponent produces a destabilizing moment of 53.4 N·cm about the rear axle, while the robot’s own weight provides only 26.7 N·cm of stabilizing moment—a deficit of 26.7 N·cm that the tail must supply by pressing down behind the rear axle.

The tail actuator uses a compact 12 V DC gearmotor driving a 2 mm pitch lead-screw linear actuator connected to the tail pitch joint via a crank linkage. The lead-screw mechanism provides high mechanical advantage and is self-locking under load, meaning the tail maintains bracing pressure even if the motor is momentarily de-energized. A dedicated tail actuator driver PCB provides an H-bridge power stage with current sensing (10 mΩ shunt + amplifier) for stall protection and a thermistor (NTC 10kΩ) for thermal monitoring. Limit switches at both ends of travel prevent over-extension. The tail tip accepts interchangeable modules: a jab/pusher tip, a hook tip for grabbing, and a high-friction rubber brace foot for ground contact.

This subsystem interfaces with Subsystem 4 (PWM/DIR commands and GPIO/ADC sensor feedback from ESP32) and Subsystem 5 (V_{bat} power and dedicated driver stage).

Figure 6: Scorpion Tail Stinger Mechanism and Anti-Tip Torque Balance

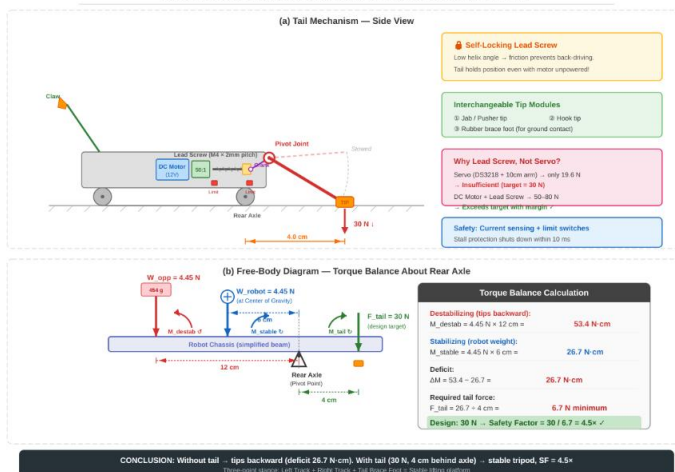


Table 3: Subsystem 3 — Scorpion Tail Stinger Requirements & Verification

| Requirements | Verification |
|---|--|
| The tail shall prevent the chassis from tipping backward when the front arms lift a 454 g load. | This requirement can be verified by commanding both arms to lift a 454 g weight while the tail is deployed in brace mode. If the chassis remains within 45° of horizontal during the lift in 3 out of 3 trials, we have successfully fulfilled this requirement. |
| The tail shall transition from stowed to bracing position in ≤ 1.0 second. | This requirement can be verified with a phone stopwatch. We will command the tail from stowed to full brace and time the motion. If the transition completes within 1.0 second, we have successfully fulfilled this requirement. |

2.6 Subsystem 4 — Wireless Control and Main Controller

An ESP32-WROOM-32E-N4 module serves as the central MCU, providing Wi-Fi and BLE connectivity, PWM generation for all actuators, I²C bus management for sensors (INA219 battery monitor, thermistors), and GPIO for limit switches and encoders. The operator uses a BLE gamepad (e.g., 8BitDo Zero 2) or a custom Wi-Fi UDP control application running on a smartphone or laptop. The ESP32 firmware is written in C/C++ using the ESP-IDF framework.

A heartbeat failsafe monitors incoming command packets. If no valid packet arrives within 500 ms, the firmware commands all motors to coast (not brake, to avoid jolting if the robot is moving) and all actuators to relax to safe stowed positions. The ESP32 also aggregates and transmits telemetry data (battery voltage, motor currents, MOSFET/motor temperatures) back to the operator device at 5 Hz.

This subsystem satisfies the third high-level requirement (wireless range, latency, and failsafe) and interfaces with all other subsystems as the central control and telemetry hub.

Figure 7: ESP32 Firmware State Machine Diagram

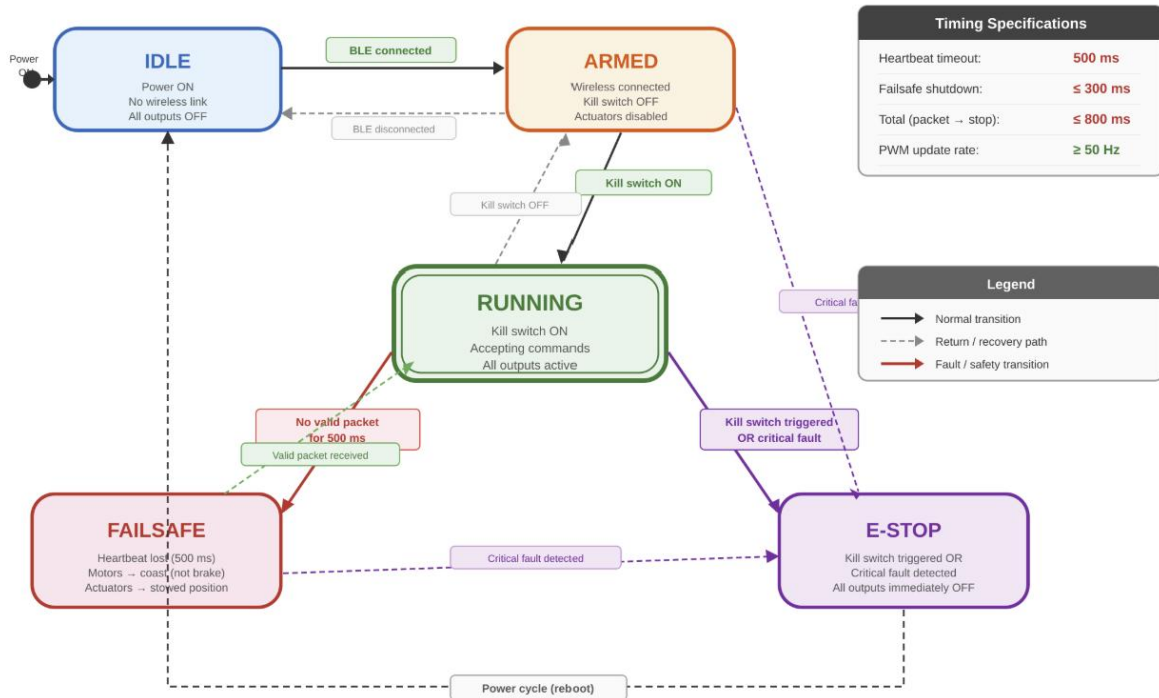


Table 4: Subsystem 4 — Wireless Control Requirements & Verification

| Requirements | Verification |
|---|---|
| The wireless link (BLE or Wi-Fi) shall maintain a stable connection at up to 10 m line-of-sight. | This requirement can be verified with a measuring tape. We will position the controller 10 m away from the robot and command all motors and actuators. If the robot responds correctly to all commands at this distance, we have successfully fulfilled this requirement. |
| The heartbeat failsafe shall disable all motor and actuator outputs within 500 ms of signal loss. | This requirement can be verified by intentionally disconnecting the controller during operation and timing how long the robot takes to stop all motion. If the robot disables within 500 ms of disconnection, we have successfully fulfilled this requirement. |

2.7 Subsystem 5 — Power, Safety, and Compliance

A 3S LiPo battery (11.1 V nominal, ≈ 1000 mAh, 15C or higher discharge rate) provides the main energy source. The power distribution board includes a physical kill switch (removable arming plug) accessible from outside the chassis for competition compliance, a 20 A blade fuse on the main positive rail, TVS diodes (bidirectional, 15 V clamping) for transient suppression from motor inductive kickback, and a Schottky diode for reverse-polarity protection. An INA219 I²C current/voltage monitor on the main rail provides continuous telemetry to the ESP32.

Separate buck regulators produce two regulated rails: 5 V at 3 A (for servo power and actuator logic, using a TPS5430 or equivalent) and 3.3 V at 500 mA (for ESP32 and sensor logic, using an AMS1117-3.3 LDO from the 5 V rail). The 5 V servo rail includes 1000 μ F of bulk electrolytic capacitance to handle servo inrush current. LiPo-safe practices are enforced: firmware low-voltage cutoff at 3.3 V/cell (9.9 V total), charging only in approved fireproof bags with a balance charger, and current limiting on all high-current loads.

This subsystem interfaces with all other subsystems by supplying power and reporting battery state.

Figure 8: Power Distribution Schematic

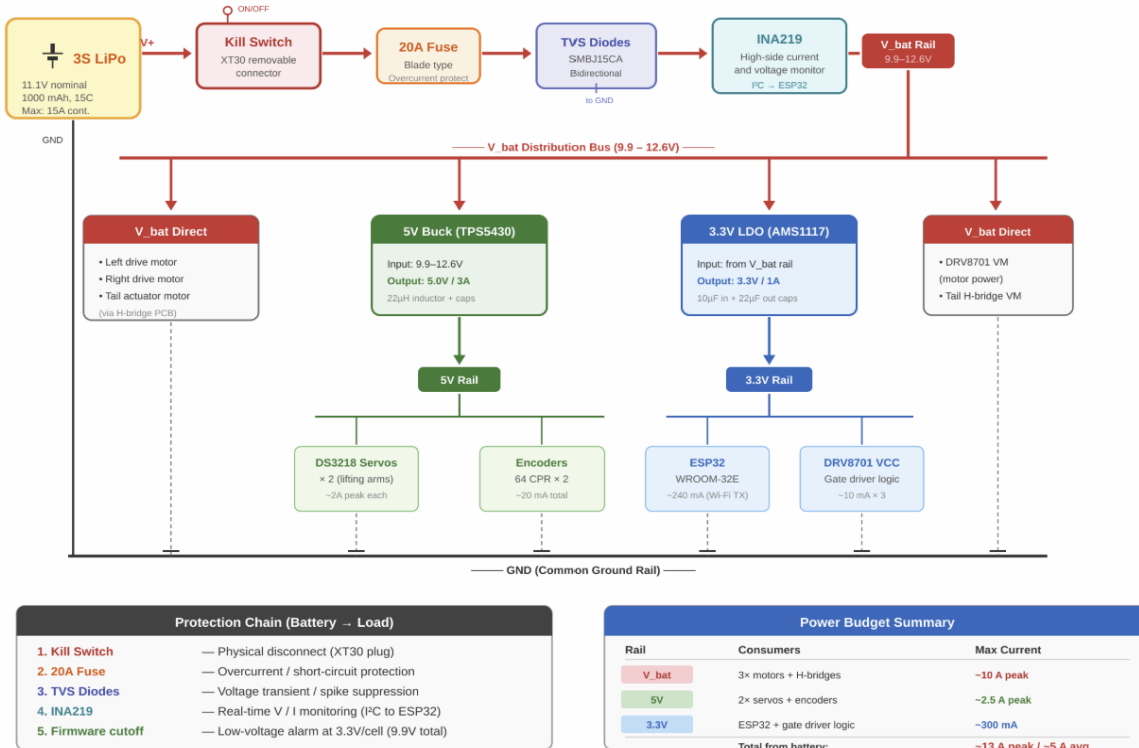


Table 5: Subsystem 5 — Power, Safety, and Compliance Requirements & Verification

| Requirements | Verification |
|--|--|
| Voltage regulation must maintain 3.3 V ±5% for the ESP32 under all load conditions. | This requirement can be verified utilizing a multimeter. We will measure the voltage at the 3.3 V regulator output while operating all motors and actuators at various speeds. If the voltage remains within 3.3 V ±5%, we have successfully fulfilled this requirement. |
| The battery shall supply sufficient current to run all subsystems for at least 2 minutes continuously. | This requirement can be verified by running the robot with all subsystems active (driving, lifting, tail bracing) for the full duration of a typical match. If the robot operates for the complete 2-minute duration without voltage sag or shutdown, we have successfully fulfilled this requirement. |

2.8 Tolerance Analysis

We identify three critical feasibility risks and analyze each quantitatively: (1) arm lifting force, (2) arm structural strength, and (3) tail anti-tip stability. Together, these analyses demonstrate that the design can lift a full ant-weight opponent while remaining stable. The tolerance analysis was selected in consultation with our TA as the most critical interface to the success of the project, because the lifting-while-stable function requires all three analyses to pass simultaneously.

2.8.1 Arm Lifting Force Feasibility

Risk: Can each arm actually lift a full 454 g ant-weight opponent? If not, the second high-level requirement fails.

Servo specification: The DS3218 servo produces $20 \text{ kg}\cdot\text{cm} = 1.96 \text{ N}\cdot\text{m}$ of torque at the horn at 6.0 V supply.

Four-bar linkage geometry: The input crank (servo horn) has a radius of 2.5 cm. The output crank (arm contact point) has a radius of 4.0 cm. The effective arm length from the linkage output pivot to the claw tip is 8.0 cm. At the mid-stroke position, the linkage provides a mechanical advantage (MA) of approximately 1.5 \times .

Calculated force per arm:

$$F_{\text{tip}} = (\tau_{\text{servo}} / L_{\text{arm}}) \times \text{MA} = (1.96 \text{ N}\cdot\text{m} / 0.08 \text{ m}) \times 1.5 = 36.8 \text{ N} \text{ (3.75 kg)}$$

$$\text{Two arms combined: } 2 \times 36.8 = 73.6 \text{ N (7.50 kg)}$$

$$\text{Opponent weight: } 0.454 \text{ kg} \times 9.81 = 4.45 \text{ N}$$

$$\text{Safety factor per arm: } 36.8 / 4.45 = 8.3\times$$

Conclusion: Each arm alone can lift more than 8 times the opponent weight. Even accounting for friction losses, imperfect linkage angles, and dynamic loading, the margin is very large.

2.8.2 Arm Structural Material Selection

Risk: Will the arm linkage members break or deform under load?

Loading condition: Each arm linkage member is modeled as a cantilever beam with a tip load of 36.8 N and a free length of 8.0 cm. **Cross-section:** 18 mm wide \times 8 mm thick (PLA+, 3D-printed, 100% infill).

$$\text{Bending moment at root: } M = F \times L = 36.8 \times 0.08 = 2.94 \text{ N}\cdot\text{m}$$

$$\text{Section modulus: } S = bh^2/6 = (18 \times 8^2) / 6 = 192 \text{ mm}^3 = 1.92 \times 10^{-7} \text{ m}^3$$

$$\text{Peak bending stress: } \sigma = M / S = 2.94 / 1.92 \times 10^{-7} = 15.3 \text{ MPa}$$

Table 6: Material Comparison for Arm Linkage Members at 15.3 MPa Peak Stress

(18 mm × 8 mm cross-section)

| Material | Yield Strength (MPa) | Safety Factor | Verdict |
|------------------|----------------------|---------------|---|
| PLA+ (Tough PLA) | 55 | 3.6× | SELECTED |
| Standard PLA | 60 | 3.9× | Rejected — brittle under impact |
| PETG | 50 | 3.3× | Backup option |
| ABS | 40 | 2.6× | Rejected — warping, fumes |
| Nylon (PA6) | 55 | 3.6× | Rejected — hygroscopic, harder to print |

Conclusion: PLA+ is selected for all structural arm linkage members with an enlarged cross-section of 18 mm × 8 mm (increased from the aluminum baseline of 15 mm × 6 mm). The 3.6× safety factor is sufficient for the ant-weight class, where impact loads are moderate. PLA+ offers superior toughness over standard PLA (resists shattering on impact), is the most widely available FDM filament, and enables rapid design iteration. Despite the larger cross-section, PLA+ members are lighter than aluminum equivalents (0.179 g/mm vs. 0.243 g/mm) due to its low density (1.24 g/cm³). Standard PLA was rejected because it is brittle and may shatter under repeated combat impacts.

2.8.3 Tail Anti-Tip Torque Balance

Risk: When the front arms lift an opponent, the reaction force tips the robot backward. If the tail cannot counteract this moment, the robot flips itself.

Free-body analysis (moments about the rear axle ground contact):

Robot mass: 454 g → weight $W_r = 4.45$ N

Robot CG: 6.0 cm forward of rear axle

Arm lift point: 12.0 cm forward of rear axle

Opponent weight: $W_{opp} = 4.45$ N

Tail contact point: 4.0 cm behind rear axle

Stabilizing moment: $M_{stable} = W_r \times d_{CG} = 4.45 \times 0.06 = 0.267$ N·m = 26.7 N·cm

Destabilizing moment: $M_{destab} = W_{opp} \times d_{arm} = 4.45 \times 0.12 = 0.534$ N·m = 53.4

N·cm

Moment deficit: $\Delta M = 53.4 - 26.7 = 26.7 \text{ N}\cdot\text{cm}$

Required tail downforce: $F_{\text{tail}} = \Delta M / d_{\text{tail}} = 26.7 / 4.0 = 6.7 \text{ N}$

Design target: 30 N \rightarrow Anti-tip safety factor = $30 / 6.7 = 4.5\times$

Actuator comparison: A DS3218 servo on a 10 cm tail arm produces only 19.6 N (1.96 N·m / 0.10 m)—short of the 30 N target. The DC gearmotor + lead-screw combination produces 50–80 N, comfortably exceeding the target. The lead screw’s self-locking property eliminates continuous motor current during sustained bracing.

Conclusion: The torque balance confirms the robot will tip backward without the tail. With 30 N at 4 cm behind the rear axle, the system has a 4.5× anti-tip safety margin.

3. Cost and Schedule

3.1 Cost Analysis

3.1.1 Labor

Assuming a starting salary of \$85,000/year for an ECE graduate from UIUC (approximately \$42.50/hour), and applying the standard 2.5× multiplier:

Per team member: $\$42.50/\text{hr} \times 2.5 \times 60 \text{ hours} = \$6,375$

Total labor (3 members): $\$6,375 \times 3 = \$19,125$

3.1.2 Parts

Table 7: Itemized Parts List

| Description | Manufacturer | Part # | Qty | Unit Cost | Extended |
|--|--------------|--------|-----|-----------|----------|
| Pololu 100:1 Metal Gearmotor w/ 64 CPR Encoder | Pololu | 4844 | 2 | \$25.00 | \$50.00 |
| Pololu 30T Track Set (pair) | Pololu | 3032 | 1 | \$20.00 | \$20.00 |
| DS3218 High-Torque Metal Gear Servo (20 kg·cm) | DSSERVO | DS3218 | 2 | \$12.00 | \$24.00 |
| 12V DC Gearmotor (50:1) for Lead Screw | Pololu | 4754 | 1 | \$18.00 | \$18.00 |

| | | | | | |
|--|-------------------|-----------------|----|---------|---------|
| M4×2mm Lead Screw + Nut Assembly (100mm) | Generic | — | 1 | \$8.00 | \$8.00 |
| ESP32-WROOM-32E-N4 Module | Espressif | ESP32-WROOM-32E | 2 | \$4.00 | \$8.00 |
| TI DRV8701 Gate Driver IC | Texas Instruments | DRV8701E | 4 | \$2.50 | \$10.00 |
| IRLR7843 N-MOSFET (D-PAK) | Infineon | IRLR7843 | 16 | \$0.80 | \$12.80 |
| INA219 I ² C Current/Voltage Monitor Breakout | Adafruit | 904 | 2 | \$10.00 | \$20.00 |
| 3S LiPo Battery 11.1V 1000mAh 25C | Turnigy | N1000.3S.25 | 2 | \$15.00 | \$30.00 |
| TPS5430 5V 3A Buck Regulator (+ passives) | Texas Instruments | TPS5430 | 2 | \$3.00 | \$6.00 |
| AMS1117-3.3 LDO Regulator | AMS | AMS1117-3.3 | 3 | \$0.50 | \$1.50 |
| PLA+ Filament (1 kg spool) | eSUN | PLA+1KG | 1 | \$25.00 | \$25.00 |
| PETG Filament (1 kg spool) | Hatchbox | 3D-PETG-1KG | 1 | \$23.00 | \$23.00 |
| Custom PCB Fabrication (3 boards, 2 copies each) | JLPCB | — | 1 | \$30.00 | \$30.00 |
| Passive Components (resistors, caps, diodes, connectors) | Various | — | 1 | \$40.00 | \$40.00 |
| NTC 10kΩ Thermistors | Generic | — | 3 | \$1.00 | \$3.00 |
| Limit Switches (micro lever) | Generic | — | 4 | \$0.50 | \$2.00 |
| TVS Diodes (SMBJ15CA) | Vishay | SMBJ15CA | 4 | \$0.60 | \$2.40 |
| 20A Blade Fuse + Holder | Generic | — | 2 | \$2.00 | \$4.00 |
| XT30 Connectors (kill switch plug) | Generic | — | 4 | \$1.00 | \$4.00 |
| Misc Hardware (screws, standoffs, wiring, heat shrink) | Various | — | 1 | \$25.00 | \$25.00 |
| 8BitDo Zero 2 BLE Gamepad | 8BitDo | Zero2 | 1 | \$20.00 | \$20.00 |

Parts Subtotal: \$376.70

Shipping (est. 5%): \$18.84

Sales Tax (est. 10%): \$37.67

Total Parts Cost: \$433.21

Machine Shop Services: Estimated 1 hour at \$50/hr = \$50.00 (chassis drilling and minor modifications only; arm linkages are 3D-printed)

Grand Total: \$19,125 (labor) + \$433.21 (parts) + \$250.00 (shop) = \$19,808.21

3.2 Schedule

Figure 9: Project Schedule — Gantt Chart (10-Week Timeline)

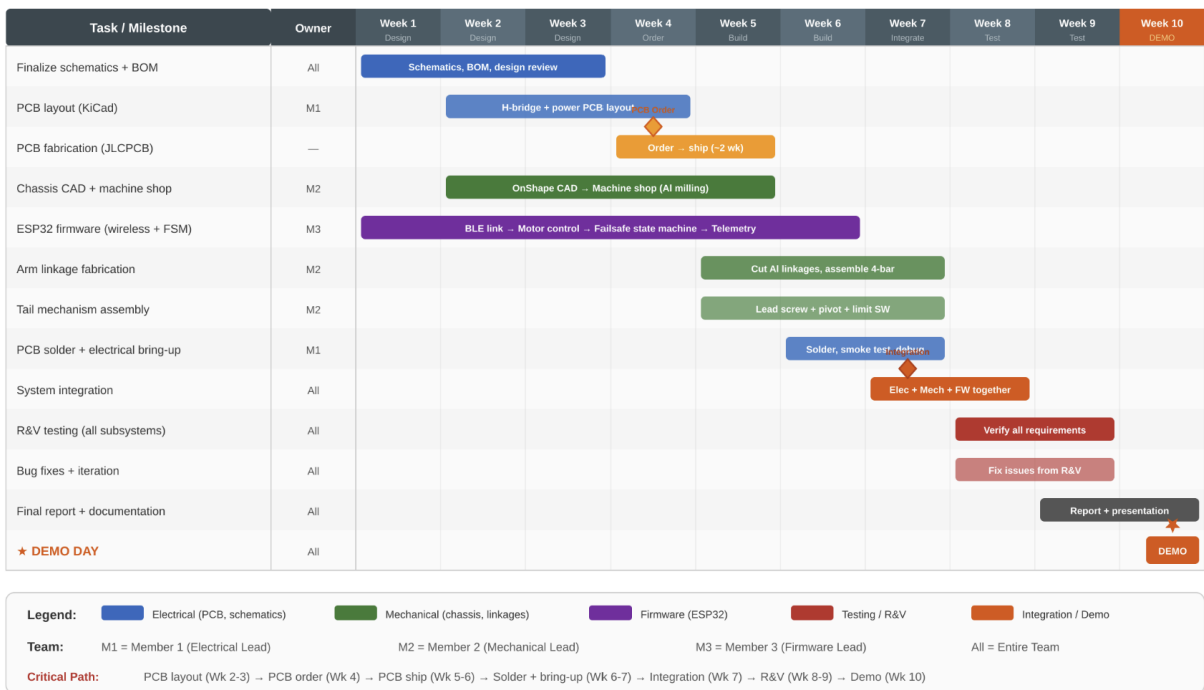


Table 8: Project Schedule

| Week | Tasks | Person(s) |
|-----------------------|--|--|
| Week 1 (Feb 16–22) | Finalize design document, order all parts, begin CAD modeling | All |
| Week 2 (Feb 23–Mar 1) | PCB schematic design (H-bridge, tail driver, power board); begin 3D printing arm linkages (PLA+) | Zixin: PCB Chen: Mech Zisu: Firmware |
| Week 3 (Mar 2–8) | PCB layout and design review; 3D print chassis prototype; begin ESP32 firmware (BLE, PWM) | Zixin: PCB Chen: 3D print Zisu: Firmware |
| Week 4 (Mar 9–15) | ORDER PCBs; assemble mechanical prototype (tracks, arms, tail); test servos and gearmotors on breadboard | All |

| | | |
|-----------------------|---|-------------------------------------|
| Week 5 (Mar 16–22) | Receive and solder PCBs; individual subsystem bench testing (H-bridge, tail driver, power) | Zixin: Solder Chen: Mech Zisu: Test |
| Week 6 (Mar 23–29) | Integrate drive electronics with tracks; integrate servos with arm linkages; tail actuator assembly | All |
| Week 7 (Mar 30–Apr 5) | Full system integration; wireless control testing; failsafe verification | All |
| Week 8 (Apr 6–12) | R&V testing for all subsystems; iterate on issues; PCB revision if needed | All |
| Week 9 (Apr 13–19) | Final integration testing; self-righting tests; endurance/thermal tests | All |
| Week 10 (Apr 20–26) | Prepare demo; final debugging; practice demo runs | All |
| Demo Week | Final demonstration | All |

4. Discussion of Societal Impact, Engineering Standards, Ethics, and Safety

4.1 Societal Impact

This project contributes positively to engineering education by demonstrating the integration of custom power electronics, embedded control, and mechanical design in a compact, weight-constrained platform. The skills developed—custom PCB design, motor control, wireless telemetry, and thermal management—are directly transferable to industries including autonomous vehicles, industrial automation, and assistive robotics. The tracked mobility platform with self-righting capability has potential applications in search-and-rescue and inspection robotics where terrain traversal and flip recovery are critical.

From an environmental perspective, the project uses a rechargeable LiPo battery (reducing disposable battery waste) and minimizes material waste by using 3D printing (PLA+ and PETG) for both structural arm linkages and non-structural components, eliminating the need for subtractive aluminum machining. All electronic components and batteries will be responsibly recycled or disposed of at the end of the project per UIUC hazardous waste guidelines.

4.2 Engineering Standards

The following standards apply to this project:

IPC-2221B (Generic Standard on Printed Board Design) [6]: All custom PCBs will be designed with appropriate trace widths for current carrying capacity, creepage and clearance distances for the 12 V power rail, and thermal relief pads for power components.

UL 1642 (Lithium Batteries): The LiPo battery usage follows standard safety practices including charge control, over-discharge protection, and current limiting.

FCC Part 15 (Unintentional Radiators): The ESP32 module is FCC-certified. The custom PCB design will minimize EMI through proper grounding and decoupling.

ANSI/UL 1244 (Electrical and Electronic Measuring and Testing Equipment): All test equipment used during verification will be calibrated and operated according to manufacturer specifications.

4.3 Ethical Considerations

As engineers, we are bound by the IEEE Code of Ethics [3] to hold paramount the safety, health, and welfare of the public. Although combat robots operate against other robots in a controlled arena, there is inherent risk of injury from high-speed

mechanisms, high-current electrical systems, and lithium-polymer batteries.

IEEE Code Section I.1 (Safety of the Public): We mitigate risks by implementing a physical kill switch, overcurrent protection on all motor channels, and a wireless heartbeat failsafe. All testing will follow ECE 445 lab safety protocols including safety glasses and a controlled test enclosure [3].

IEEE Code Section I.5 (Honest Representation): We will not falsely claim that our safety features prevent all accidents. The robot mitigates some hazards but does not eliminate the inherent risks of combat robotics. We will be honest about the system's capabilities and limitations [3].

IEEE Code Section I.7 (Avoiding Conflicts of Interest): This project is academic with no commercial conflicts. All design decisions are made on engineering merit. We will credit all third-party designs, open-source code, and reference materials [3].

ACM Code of Ethics Section 1.2 (Avoid Harm): The robot is a non-destructive control bot with no spinning weapons, inherently reducing the risk of projectile debris and catastrophic damage compared to spinner-class robots [4].

4.4 Safety Considerations and Mitigation

4.4.1 Lithium-Polymer Battery Hazards

LiPo batteries can catch fire or explode if punctured, overcharged, over-discharged, or short-circuited. Mitigation measures include: firmware low-voltage cutoff at 3.3 V/cell, balance charging only in fireproof bags, physical protection of the battery within the chassis, hard disconnect via kill switch, and a 20 A fuse on the main positive rail [5].

4.4.2 High-Current Electrical Hazards

The system can draw up to 15 A from the battery. All high-current conductors will be minimum 16 AWG, and the main fuse coordinates with wiring limits. TVS diodes and flyback diodes suppress inductive transients. The PCB uses appropriate creepage/clearance per IPC-2221 for the 12 V rail [6].

4.4.3 Mechanical Hazards

Moving parts (tracks, PLA+ lifting arms, tail) can cause pinch and crush injuries. The arm links carry high forces. Mitigation: the robot will be operated only in designated test areas, hands will be kept clear of mechanisms during operation, and the kill switch will be used to disable all motion before handling. The robot uses no high-energy spinning weapons, significantly reducing projectile debris risk.

4.4.4 Lab Safety Protocol

During all testing in the ECE 445 lab, we will: wear safety glasses when the robot is

powered, test within a controlled enclosure (acrylic box or arena walls), keep a fire extinguisher accessible when testing with LiPo batteries, never leave a charging LiPo unattended, and deactivate the kill switch before any physical contact with the robot.

5. Citations

- [1] Battlebots Inc., “Competition Rules and Event History,” battlebots.com, 2024.
- [2] R. Ciarcia, “Design Challenges in Small Combat Robots,” *Make Magazine*, vol. 78, pp. 42–49, 2023.
- [3] IEEE, “IEEE Code of Ethics,” ieee.org/about/corporate/governance/p7-8.html, 2024.
- [4] ACM, “ACM Code of Ethics and Professional Conduct,” acm.org/code-of-ethics, 2018.
- [5] UIUC Division of Research Safety, “Lithium Battery Safety,” drs.illinois.edu, 2024.
- [6] IPC, “IPC-2221B: Generic Standard on Printed Board Design,” 2012.
- [7] Pololu, “100:1 Metal Gearmotor 37Dx73L mm 12V with 64 CPR Encoder,” pololu.com, product #4844.
- [8] DSSERVO, “DS3218 High-Torque Servo Datasheet,” dsservo.com, 2023.
- [9] Texas Instruments, “DRV8701 Half-Bridge Gate Driver Datasheet,” ti.com, SLVSD80, 2019.
- [10] Espressif, “ESP32-WROOM-32E Datasheet,” espressif.com, v1.2, 2023.
- [11] Texas Instruments, “INA219 Bidirectional Current/Power Monitor Datasheet,” ti.com, SBOS448G, 2015.